Energy Dependence of Intermittency for Charged Hadrons in Au + Au Collisions at RHIC-STAR

Jin Wu (吴锦)[1,2]
Colloabrators: Xiaofeng Luo[1], Yufu Lin [1], Zhiming Li [1], Yuanfang Wu[1] (alphabet)

1. Key Laboratory of Quark and Lepton Physics (MOE) and Institute of Particl Physics, Central China Normal University
2. College of Physics and Electronic Engineering, Guilin University of Technology

Physics Letters B 845, 138165 (2023)，arXiv:2301.11062；
PHYSICAL REVIEW C 106, 054905 (2022)，arXiv:2209.07135.

The 15th Workshop on QCD Phase Transition and Relativistic Heavy-Ion Physics (QPT 2023)

Outline

- The QCD critical point.
- The framework of intermittency analysis.
- Results from the STAR experiment.
- Results from a hybrid UrQMD+CMC Model.
- Summary and outlook.

1.1 QCD Phase Diagram and the Critical Point

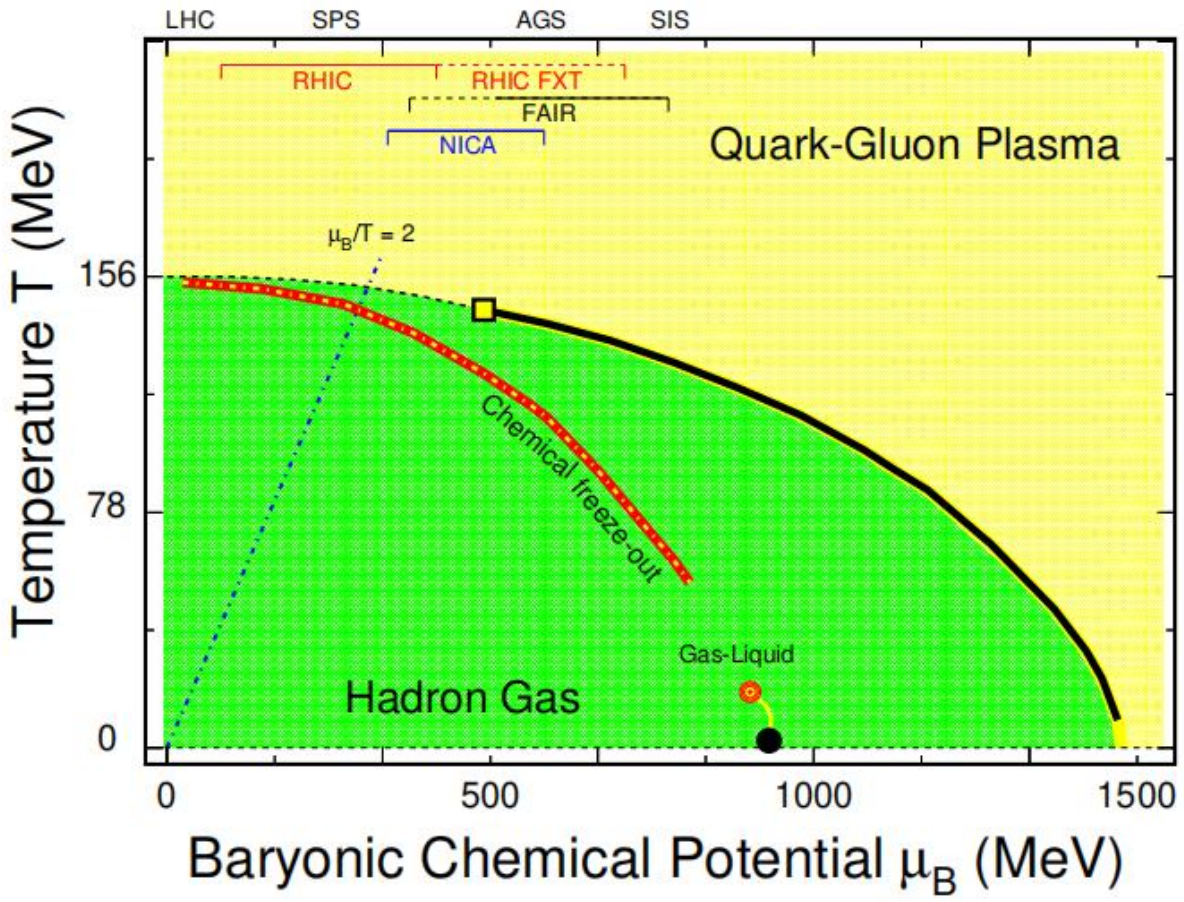

X. Luo, S. Shi, N. Xu, Y. Zhang, Particles 3, 278–307 (2020);
Bzdak, S. Esumi, V. Koch, J. Liao, M. Stepanov, N. Xu, Phys. Rept. 853, 1 (2020);
Y. Aoki, et. al., Szabo, Nature 443, 675 (2006);
S. Ejiri, Phys. Rev. D 78, 074507 (2008);
Y. Hatta and M. A. Stephanov, Phys. Rev. Lett. 91, 102003 (2003).

- Phase diagram of strongly interacting matter in T and μ_B.
- Lattice QCD calculations predicted a crossover transition from hadronic matter QGP at vanishing μ_B.
- QCD-based model calculations suggested that the phase transition is of the first-order at large μ_B
- The QCD critical point (CP): a significant point where the first-order phase transition boundary terminates.
- Upon approaching a critical point, the correlation length of the system diverges
  → A physical signature: density fluctuations.

1.2 Non-monotonic Energy Dependence of Observables in Heavy-ion Experiment

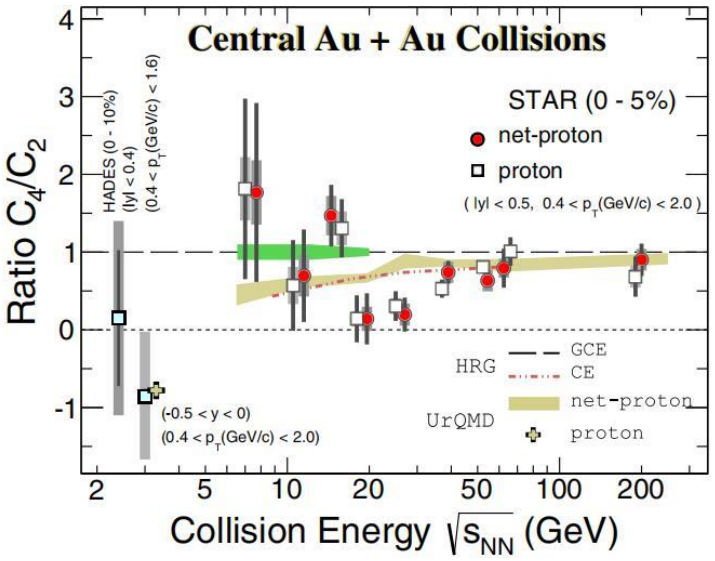

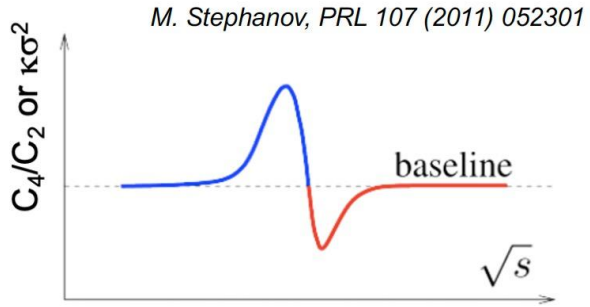

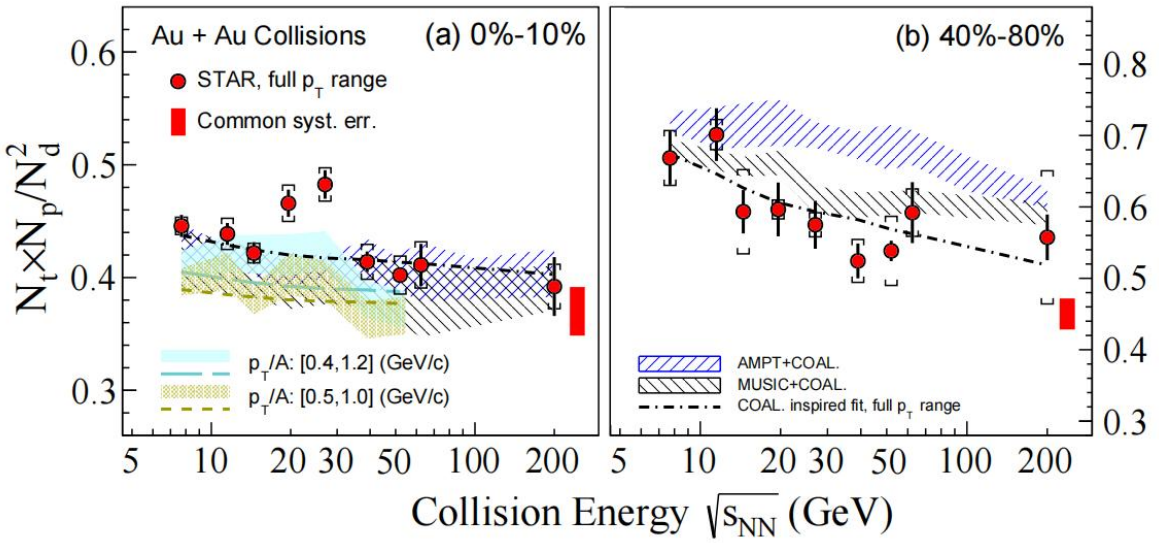

J. Adam et al. (STAR), Phys. Rev. Lett. 126, 092301 (2021);
M. S. Abdallah et al. (STAR), Phys. Rev. Lett. 128, 202303 (2022).

M. I. Abdulhamid et al. (STAR), Phys. Rev. Lett. 130, 202301 (2023).

- Non-monotonic variation with collision energy of the sensitive observables, is suggested as a possible signature for the QCD critical point.

- Several measurements from the BES program at RHIC have showed a non-monotonic energy dependence. These include the net-proton kurtosis, the yield ratio of light nuclei production …

1.3 The Framework of Intermittency Analysis

- Based on the 3D Ising-QCD calculations, the density-density function, $\rho(\kappa)$, for small momentum transfer (κ) has a power-law (self-similar) structure, which gives rise to large density fluctuations near the QCD critical point:

$$< \rho\,(k)\rho^{*}(\kappa) > \sim |k|^{-d_F}$$

N. G. Antoniou et. al, PRL 97, 032002 (2006): K.J. Sun, et.al, Phys. Lett. B 774, 103 (2017)
N. G. Antoniou, et. al, Nucl. Phys. A 693, 799 (2001).

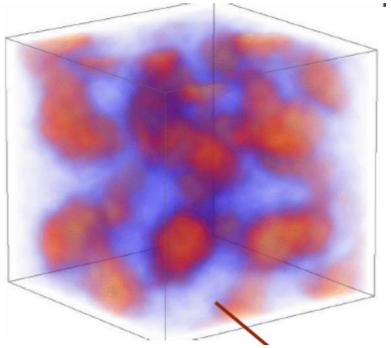

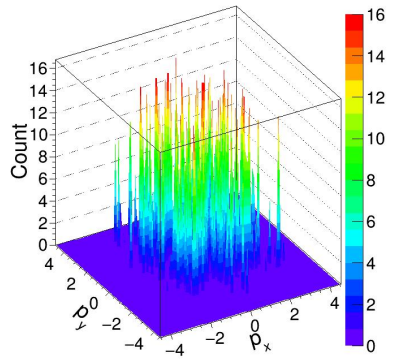

- The intermittency termed as big bursts from small region (cells) of the phase space, signals unusual density fluctuations. Critical (strong) intermittency is expected to developed near the QCD critical point.

- Density fluctuations can be probed via an intermittency analysis by utilizing the scaled factorial moments, SFMs or $F_q(M)$, defined as:

$$F_q(M) = \frac{< \frac{1}{M^D} \sum_{i=1}^{M^D} n_i(n_i-1)\dots(n_i-q+1) >}{< \frac{1}{M^D} \sum_{i=1}^{M^D} n_i >^q},$$

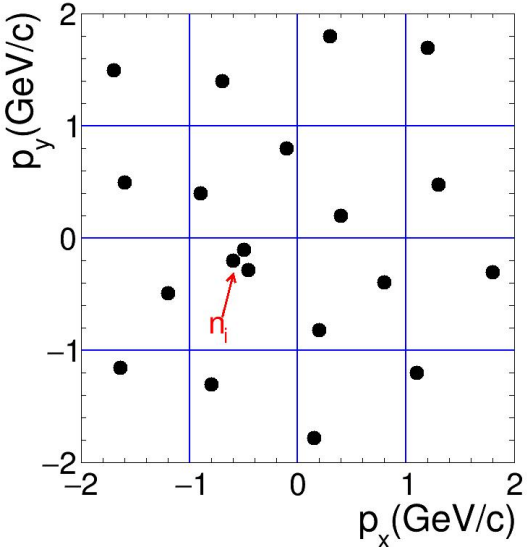

Where M^D is the number of equal-size cells in which the D-dimensional space is partitioned, q is the order of moments, $< \dots >$ denotes averaging over events.

1.4 Power-law (Scaling) Behaviors of Scaled Factorial Moments.

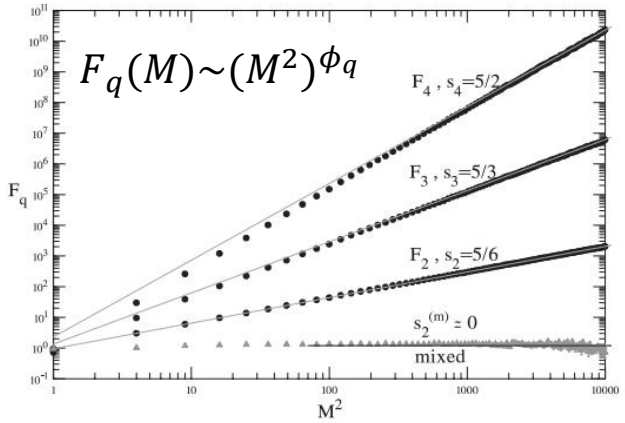

N. G. Antoniou et. al, PRL 97, 032002 (2006):
N. G. Antoniou, et. al,, NPA 761, 149 (2005).

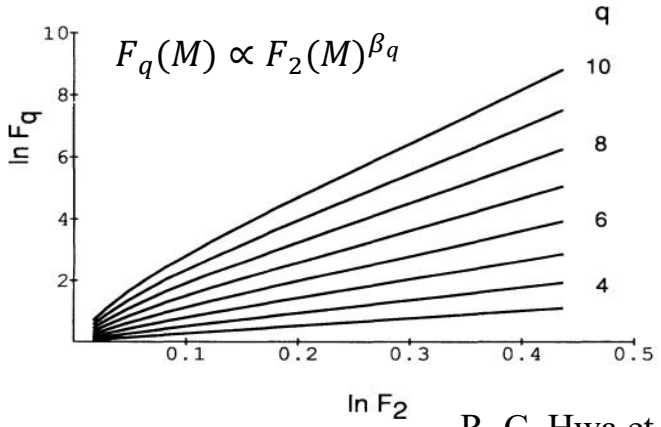

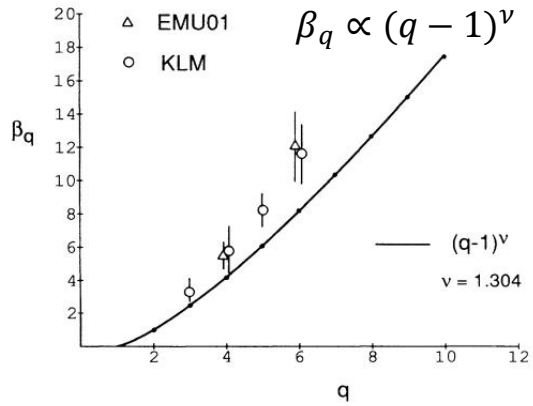

R. C. Hwa et al, PRL 69, 741 (1992); R. C. Hwa et al, PRD 47, 2773 (1993);
R. C. Hwa et al, PRC 85, 044914 (2012).

- If a system features intermittency, we expect a power-law behavior of $F_q(M)$, equivalently, $F_q(M)/M$ scaling:

$F_q(M) \propto (M^2)^{\phi_q},\ M \gg 1$

Critical intermittency near the QCD critical point : $\phi_q^{\text{critical}} = 5(q-1)/12(\text{Baryon})$
$= 2(q-1)/3(\text{pion})$

- Another type of power-law behavior, $F_q(M)/F_2(M)$ scaling: $F_q(M) \propto F_2(M)^{\beta_q}, M \gg 1$

$F_q(M)/F_2(M)$ scaling can be measured experimentally, but $F_q(M)/M$ scaling could be diluted, or washed out, during hadronic evolution.

- To describe the general consequences of the phase transition, a scaling exponent is given by:

$\beta_q \propto (q-1)^{\nu}$

Critical intermittency, ν = 1.304 (Ginzburg-Landau, entire space phase);
= 1.0 (2D Ising, entire space phase).

- The energy dependence of ν could be used to search for the signature of the critical point.

2.1 STAR Detector System && Beam Energy Scan Phase I

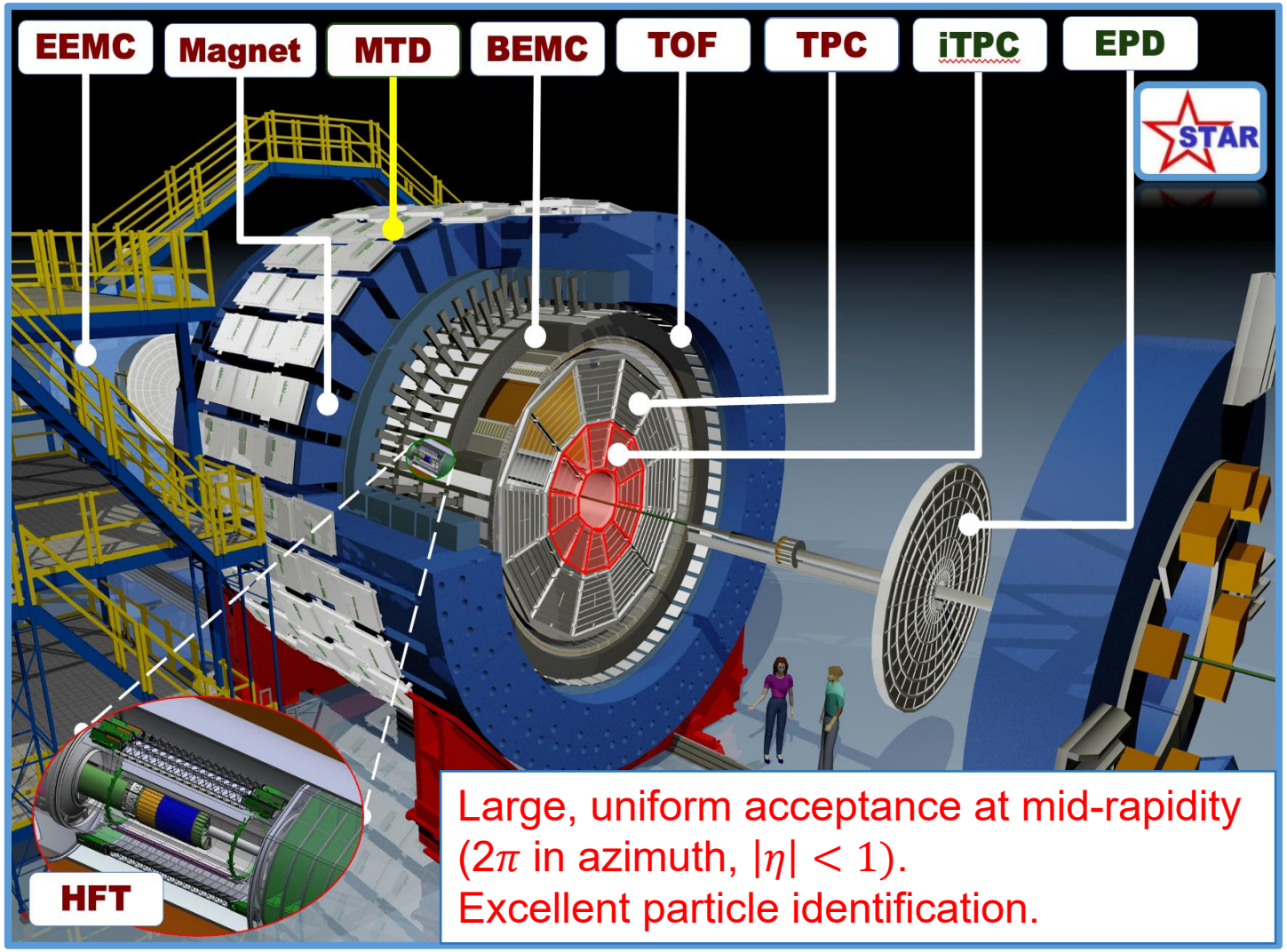

$\sqrt{s_{NN}}$ (GeV)	Year	$^*\mu_B$ (MeV)	$^*T_{CH}$ (MeV)	Events (Million)
7.7	2010	422	140	3
11.5	2010	316	152	7
14.5	2014	264	156	13
19.6	2011	206	160	16
27	2011	156	162	32
39	2010	112	164	89
54.4	2017	83	165	442
62.4	2010	73	165	47
200	2010	25	166	236

J. Cleymans et. al, PRC 73, 034905 (2006)

- Measurement of intermittency in Au + Au collisions over abroad energy range of $\sqrt{s_{NN}}$ = 7.7 - 200 GeV.

2.2 Analysis Method

- **Charged hadrons identification:**

$p, \bar{p}$	K^+, K^-	π^+, π^-
$\lvert\eta\rvert<0.5$		
$0.4<p_T<0.8$ (GeV/c)→TPC $0.4<p_T<0.8$ (GeV/c)→TPC+TOF	$0.2<p_T<0.4$ (GeV/c)→TPC $0.4<p_T<1.6$ (GeV/c)→TPC+TOF	$0.2<p_T<0.4$ (GeV/c)→TPC $0.4<p_T<1.6$ (GeV/c)→TPC+TOF

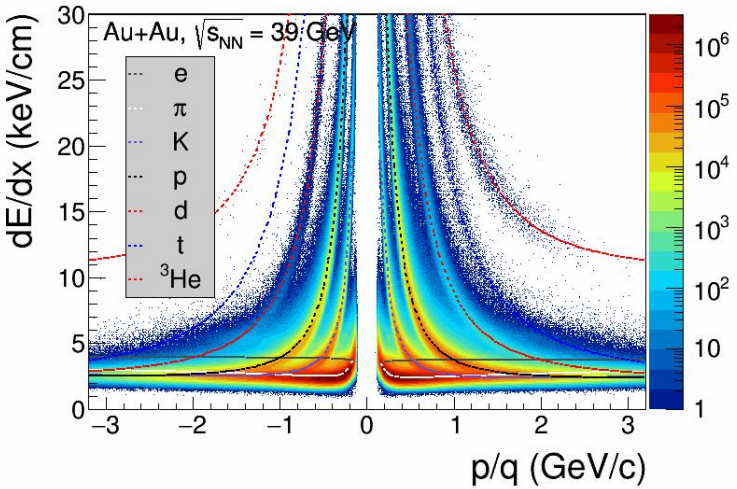

- **Centrality determination:** use charged particles ($0.5 < |\eta| < 1$) excluding particles of interest ($|\eta| < 0.5$) in order to avoid the auto-correlation.

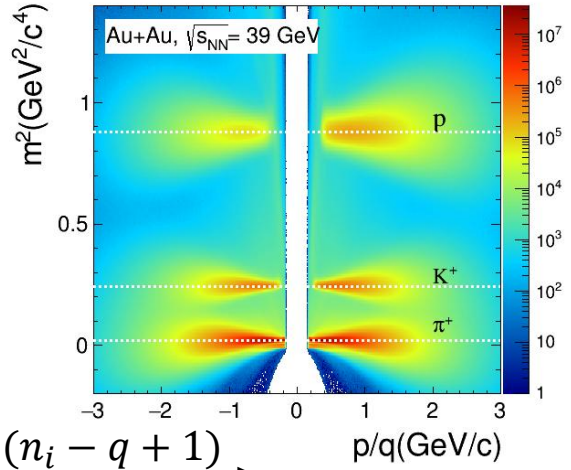

- **Mixed event method** is used to remove background and trivial fluctuations:

$$\Delta F_q(M) = F_q^{data}(M) - F_q^{mix}(M)$$

- **Efficiency correction**: cell-by-cell method.

$$F_q^{corrected}(M) = \frac{< \frac{1}{M^2} \sum_{i=1}^{M^2} \frac{n_i(n_i-1)\dots(n_i-q+1)}{\bar{\varepsilon}_i^q} >}{< \frac{1}{M^2} \sum_{i=1}^{M^2} \frac{n_i}{\bar{\varepsilon}_i} >^q}$$

- **Statistical error**: Bootstrap method.

Phys. Rev. C 104, 034902 (2021)

3.1 Results from the STAR Experiment: Energy Dependence of SFMs

$|\eta| < 0.5,\ 0.2 < p_T(K^{\pm}, \pi^{\pm}) < 1.6$ (GeV/c), $0.4 < p_T(p, \bar{p}) < 2.0$ (GeV/c)

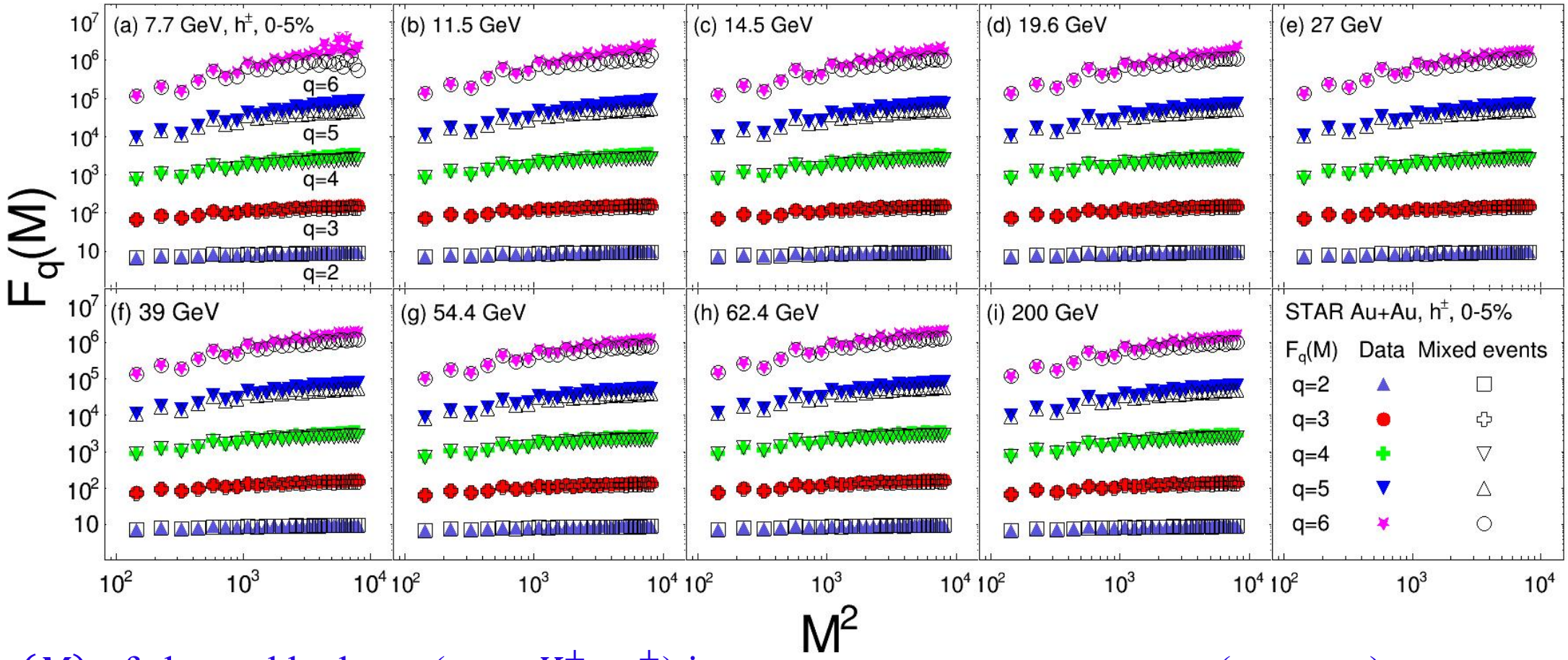

- $F_q(M)$ of charged hadrons (p, $\bar{p}$, $K^{\pm}$, $\pi^{\pm}$) in transverse momentum space ($p_x - p_y$).
- The calculations of $F_q(M)$ were performed in the $M^2 \in [1^2, 100^2]$ and up to sixth order ($q = 2{\sim}6$).
- $F_q^{data}(M)$ are larger than $F_q^{mix}(M)$ at large M^2 region.

$$\Delta F_q(M) = F_q^{data}(M) - F_q^{mix}(M).$$

3.2 Energy Dependence of $\Delta F_q(M)$ at $\sqrt{s_{\mathrm{NN}}}$ = 7.7-200 GeV

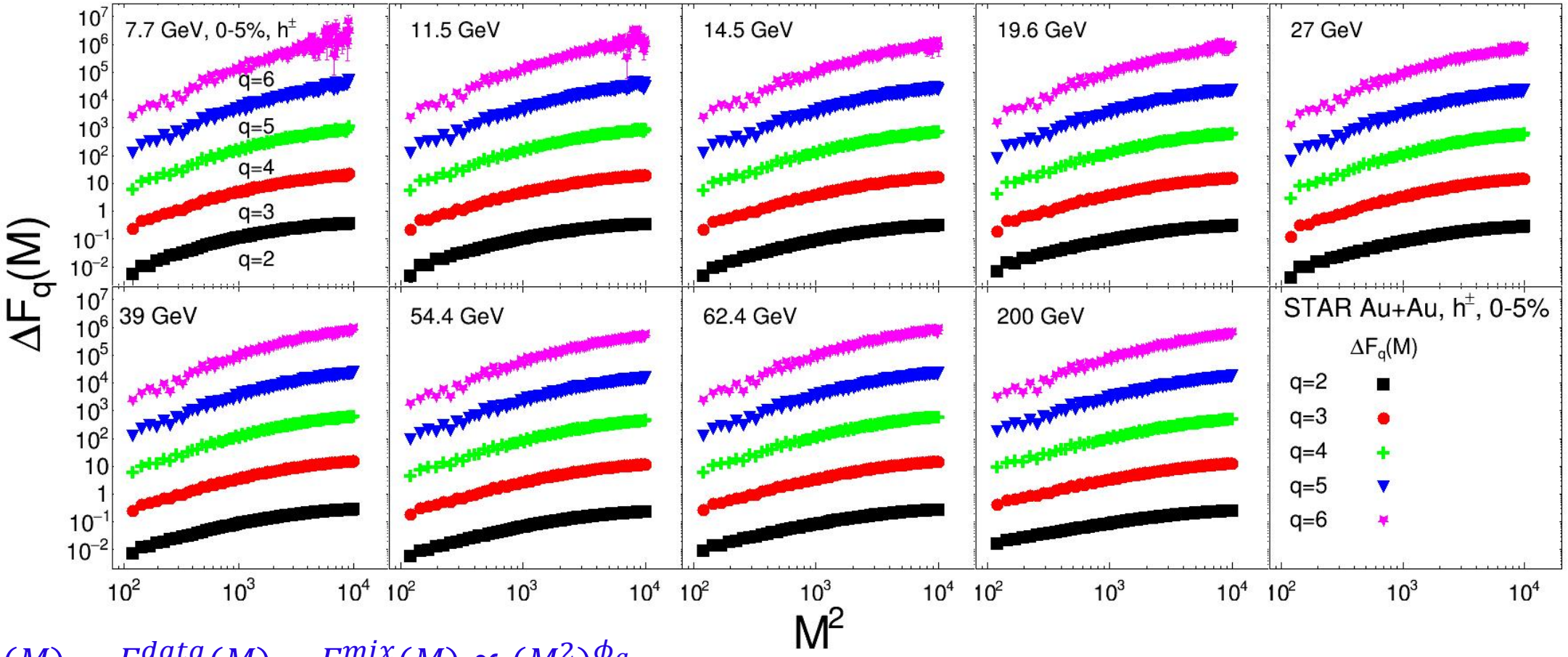

$\Delta F_q(M) = F_q^{data}(M) - F_q^{mix}(M) \propto (M^2)^{\phi_q}$

- $\Delta F_q(M)$ (q=2-6) increase with increasing M^2 and become saturated when M^2 is large (M^2 >4000) at $\sqrt{s_{\mathrm{NN}}}$ = 7.7-200 GeV . $\Delta F_q(M)$ does not obey a power-law behavior of $\Delta F_q(M) \propto (M^2)^{\phi_q}$ over the whole range of M^2. The ϕ_q cannot be extracted in a reliable manner (independently of M^2 range).

3.4 Centrality Dependence of $\Delta F_q(M)$ at $\sqrt{s_{\mathrm{NN}}}$ = 19.6 GeV

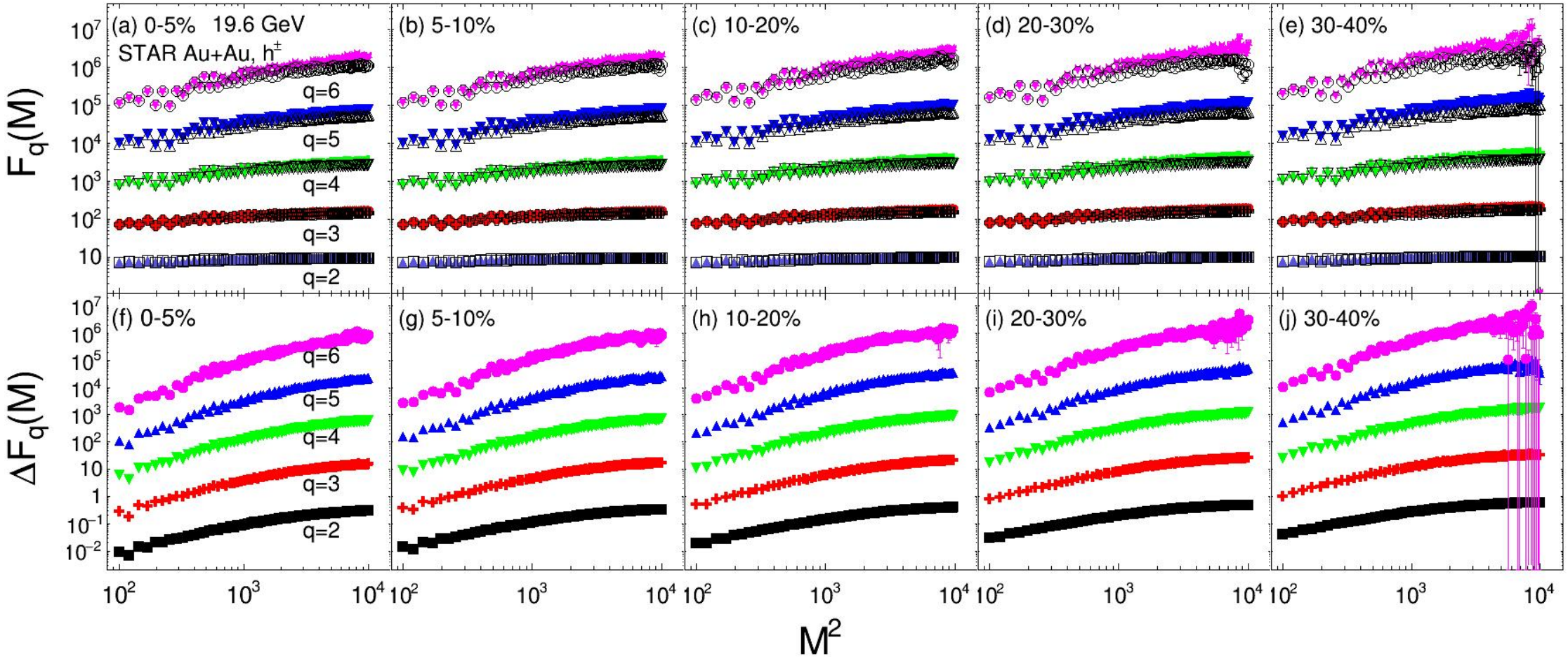

- $F_q^{data}(M)$ are larger than $F_q^{mix}(M)$ at large M^2 region in numerous mid-central collisions.

- $\Delta F_q(M)$(q=2-6) increase with increasing M^2 and become saturated when M^2 is large (M^2 >4000) in all centrality collisions. The power-law behavior of $\Delta F_q(M) \propto (M^2)^{\phi_q}$ is not observed in Au+Au collisions.

3.3 $\Delta F_q(M)$ / $\Delta F_2(M)$ Scaling in Au + Au Collisions

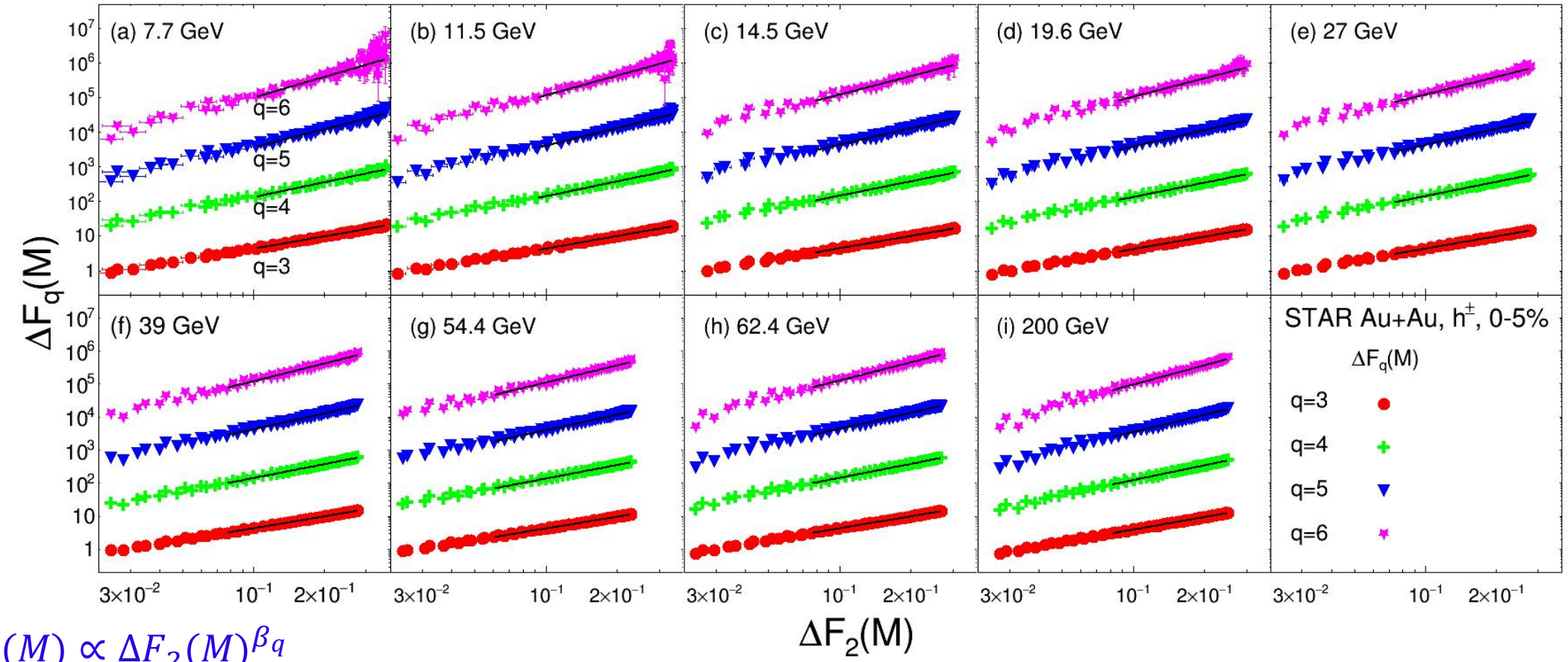

$\Delta F_q(M) \propto \Delta F_2(M)^{\beta_q}$

- $\Delta F_q(M)$ (q = 3-6) obey a strict power-law behavior with $\Delta F_2(M)$ in the most central Au+Au collisions. Clear power-law scaling of $\boldsymbol{\Delta F_q(M) \propto \Delta F_2(M)^{\beta_q}}$ is visible at all collision energies.

- The value of β_q is obtained through the best fit as the slope of the straight black line. It did not significantly change even when the fitting range was varied.

3.5 Centrality Dependence of Scaling Exponent in Au + Au Collisions

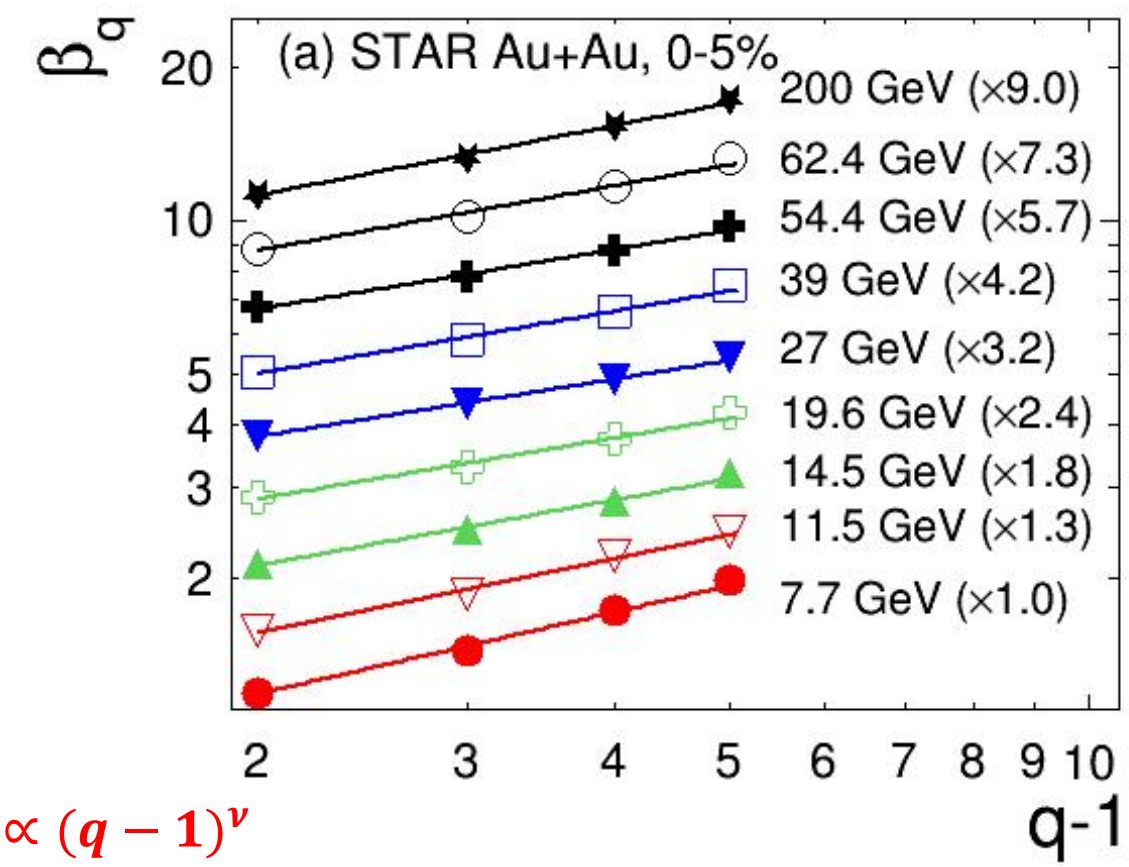

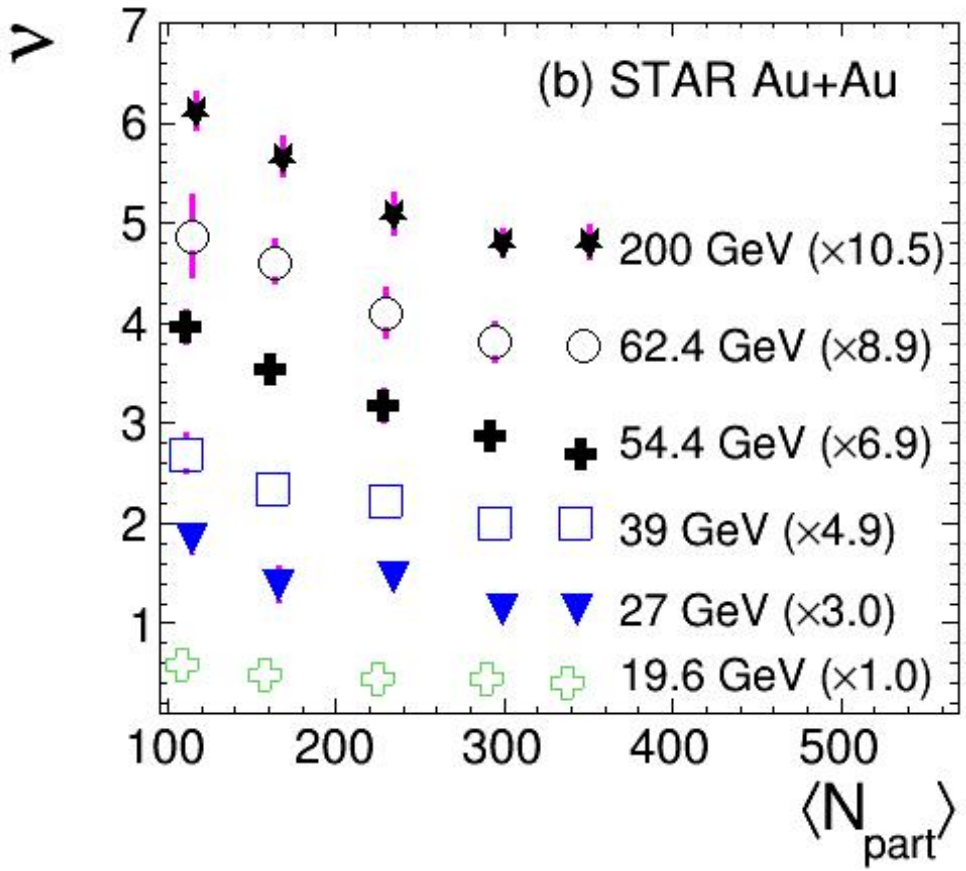

$\boldsymbol{\beta_q \propto (q-1)^{\nu}}$

- Clear power-law scaling of $\boldsymbol{\beta_q \propto (q-1)^{\nu}}$ is observed in central Au + Au collisions at $\sqrt{s_{\mathrm{NN}}}$ =7.7-200 GeV.

- ν decreases monotonically from the mid-central (30-40%) to the most central (0-5%) Au+Au collisions.

3.6 Energy Dependence of Scaling Exponent in Au + Au Collisions

$$\Delta F_q(M) \propto \Delta F_2(M)^{\beta_q}$$

$$\beta_q \propto (q-1)^{\nu}$$

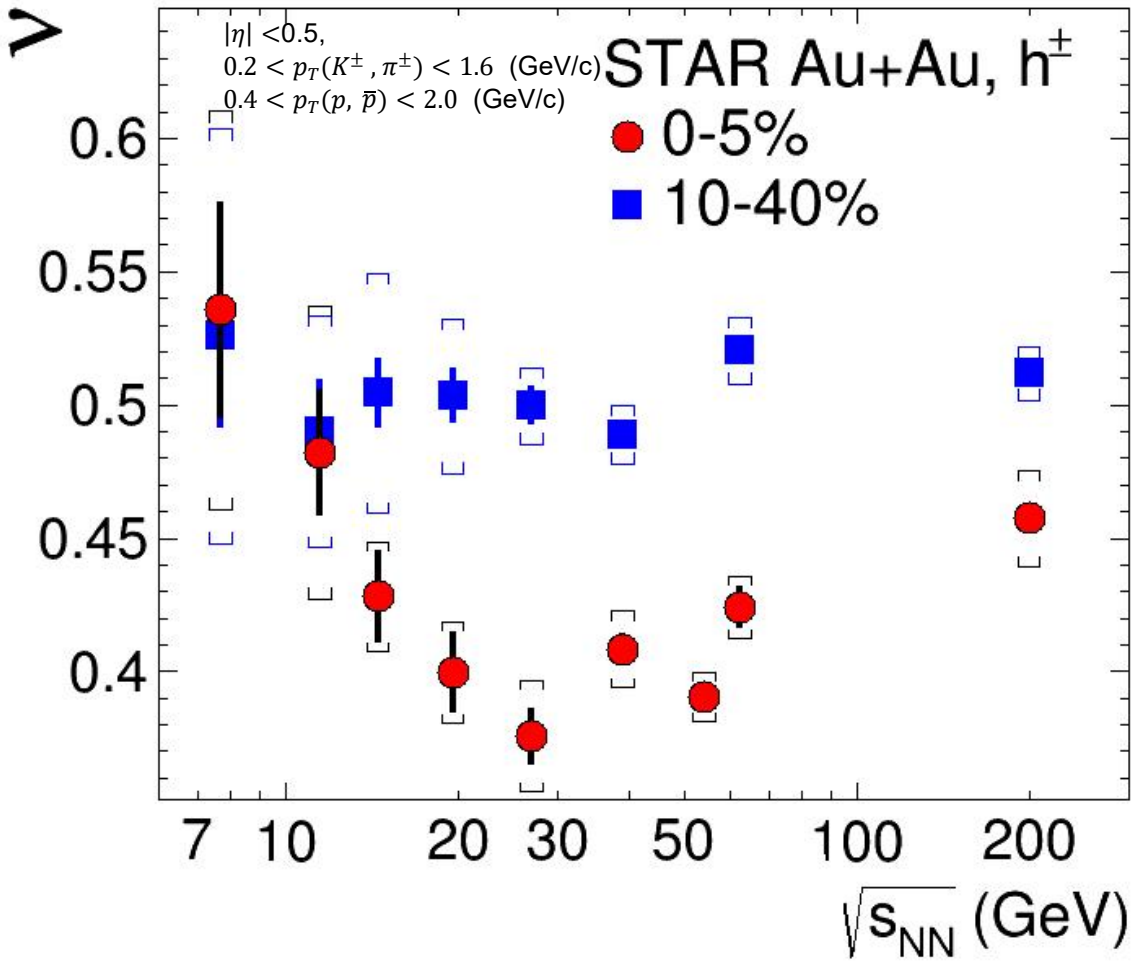

Physics Letters B 845, 138165 (2023)

- Scaling exponent (ν) exhibits a non-monotonic behavior on collision energy and seems to reach a minimum around $\sqrt{s_{NN}}$ = 20-30 GeV in the most central collisions. However, a flat energy dependence is observed in the mid-central (10-40%) collisions.

- The observed non-monotonic behavior of ν needs to be understood with more theoretical inputs.

4.1 Results from the UrQMD model: Energy Dependence of SFMs

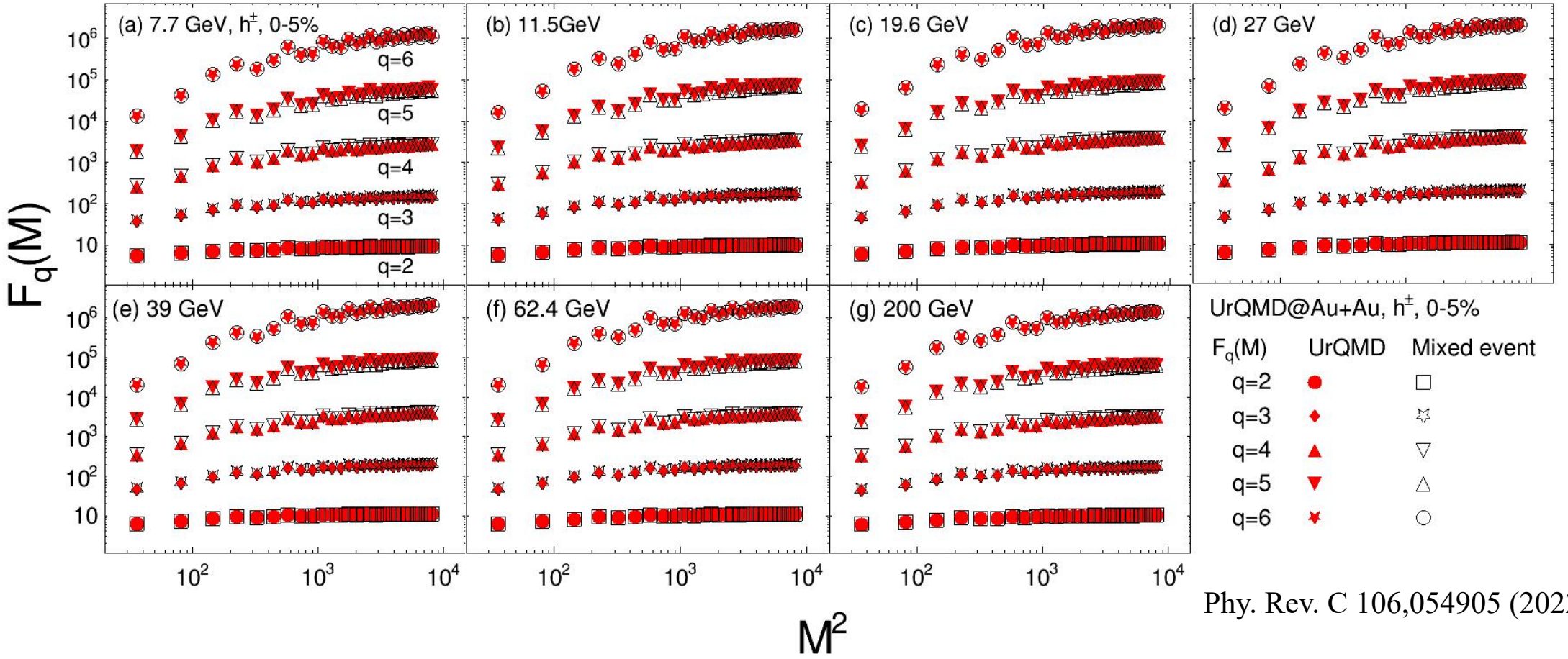

Phy. Rev. C 106,054905 (2022).

- $F_q^{data}(M)$ was observed to overlap with $F_q^{mix}(M)$ and $\Delta F_q(M) \approx 0$ from the UrQMD calculations. Neither $\Delta F_q(M) \propto (M^2)^{\phi_q}$ or $\Delta F_q(M) \propto \Delta F_2(M)^{\beta_q}$ scaling is observed after background subtraction.
- The UrQMD model fails to calculate ν due to the absence of the power-law scaling of $\Delta F_q(M) \propto \Delta F_2(M)^{\beta_q}$.

4.2 Critical Intermittency for Charged Particles from the CMC Model

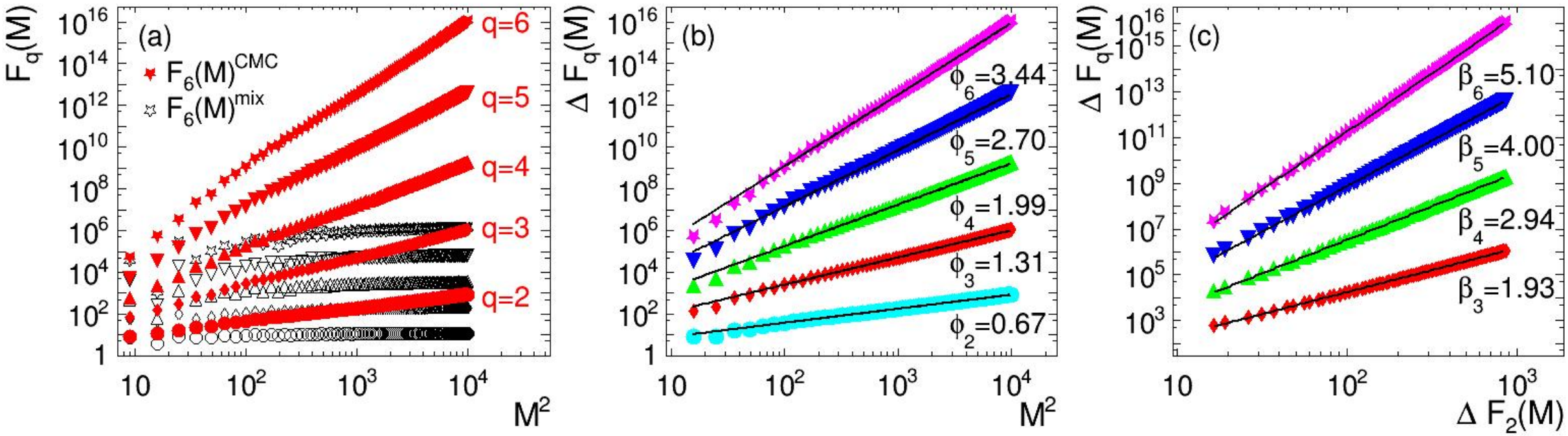

- The CMC sample which incorporates the same statistics, total multiplicity and p_T distributions as those in the UrQMD sample at $\sqrt{s_{NN}}$ = 19.6 GeV, exhibit strong power-law scaling of $\Delta F_q(M) \propto (M^2)^{\phi_q}$ and $\Delta F_q(M) \propto \Delta F_2(M)^{\beta_q}$.

- The value $\nu = 1.03 \pm 0.01$ extracted from the CMC model, is almost consist with theoretical expectation (1.0) from the 2D-Ising model calcuations.

Phys. Rev. C106, 054905 (2022)

4.3 Energy Dependence of ν from the Hybrid UrQMD+CMC Model

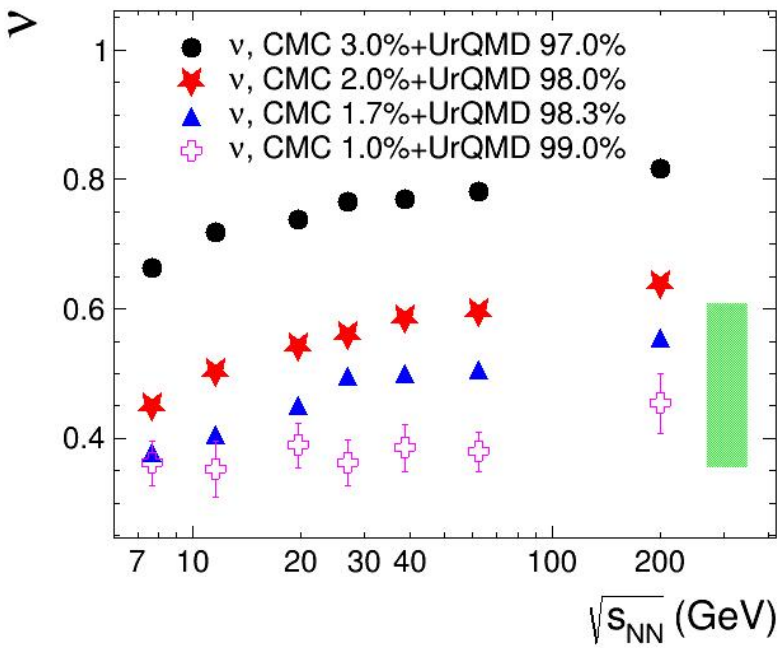

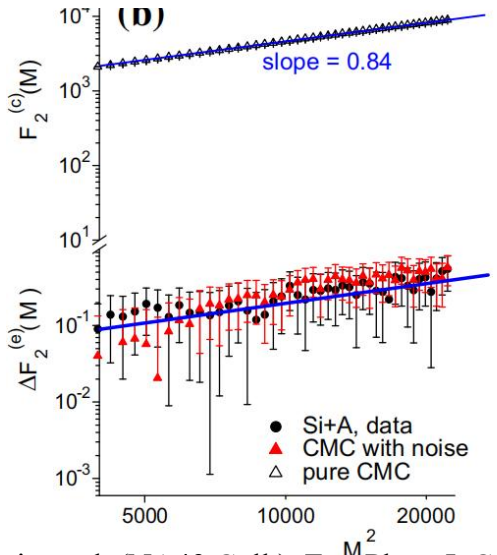

T. Anticic et al. (NA49 Coll.), Eur. Phys. J. C 75, 587 (2015).

CMC, critical $\nu = 1.03 \pm 0.01$

- As 1-2% signal of critical fluctuations from the CMC model is embedded into the UrQMD model, the energy dependence of the extracted scaling exponents show that the values are well within the experimentally measured range.
- There could exist only1-2% of intermittency signal in the central Au+Au collisions from the STAR experiment, which is similar to 1% in Si+Si collisions from the NA49 experiment.
- The current hybrid UrQMD+CMC model still fall to reproduce the observe non-monotonic energy dependence of the scaling exponnet from the STAR experiment.

5 Summary and Outlook

1) We have presented the published result of the first measurement of intermittency in heavy-ion collisions at RHIC-STAR.

1) We observed the expected power-law scaling of $\Delta F_q(M) \propto \Delta F_2(M)^{\beta_q}$ after background subtraction in Au+Au collisions at all energies.

2) Based on the scaling behavior of $\Delta F_q(M)$, the scaling exponent (ν) is extracted and found to decrease nonotonically from the peripheral to the central Au+Au collisions.

3) According to the calculations from the hybird UrQMD+CMC model, there could exist only1-2% of intermittency signal in the central Au+Au collisions from the STAR experiment, which is similar to 1% in Si+Si collisions from the NA49 experiment.

4) A non-monotonic energy dependence is observed in the 0-5% most central collisions with ν reaching a minimum around $\sqrt{s_{\mathrm{NN}}}$ = 27 GeV. Whether the observed non-monotonic behavior is related to the CEP or not, further calculations from dynamical modelling of heavy-ion collisions are required.

5 Summary and Outlook

Outlook: by utilizing data collected from the BES-II program, we will confirm the energy dependence of scaling exponent and extend the collision energy range to $\sqrt{s_{NN}}$ = 3-200 GeV.

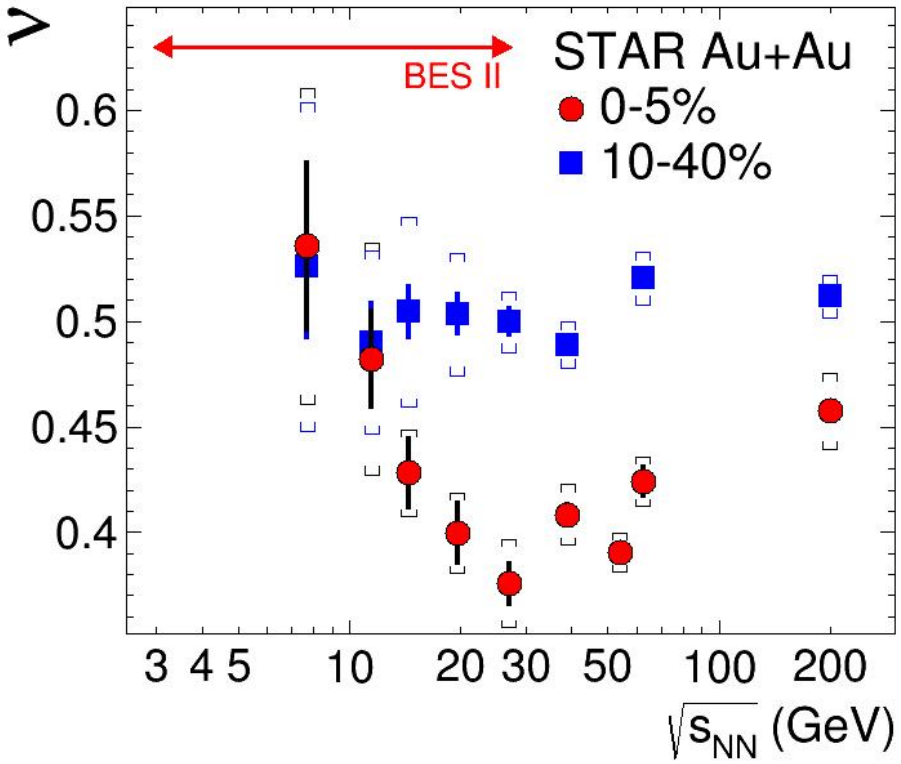

Au+Au Collisions at RHIC

Collider Runs						Fixed-Target Runs					
	$\sqrt{s_{NN}}$ (GeV)	#Events	μ_B	y_{beam}	run		$\sqrt{s_{NN}}$ (GeV)	#Events	μ_B	y_{beam}	run
1	**200**	380 M	**25** MeV	5.3	Run-10, 19	1	13.7 (100)	50 M	280 MeV	-2.69	Run-21
2	62.4	46 M	75 MeV		Run-10	2	**11.5 (70)**	50 M	320 MeV	-2.51	Run-21
3	54.4	1200 M	85 MeV		Run-17	3	**9.2 (44.5)**	50 M	370 MeV	-2.28	Run-21
4	39	86 M	112 MeV		Run-10	4	**7.7 (31.2)**	260 M	420 MeV	-2.1	Run-18, 19, 20
5	27	585 M	156 MeV	3.36	Run-11, 18	5	7.2 (26.5)	470 M	440 MeV	-2.02	Run-18, 20
6	19.6	595 M	206 MeV	3.1	Run-11, 19	6	6.2 (19.5)	120 M	490 MeV	1.87	Run-20
7	17.3	256 M	230 MeV		Run-21	7	5.2 (13.5)	100 M	540 MeV	-1.68	Run-20
8	14.6	340 M	262 MeV		Run-14, 19	8	4.5 (9.8)	110 M	590 MeV	-1.52	Run-20
9	**11.5**	57 M	316 MeV		Run-10, 20	9	3.9 (7.3)	120 M	633 MeV	-1.37	Run-20
10	**9.2**	160 M	372 MeV		Run-10, 20	10	3.5 (5.75)	120 M	670 MeV	-1.2	Run-20
11	**7.7**	104 M	420 MeV		Run-21	11	3.2 (4.59)	200 M	699 MeV	-1.13	Run-19
						12	**3.0** (3.85)	2300 M	**760** MeV	-1.05	Run-18, 21

Intermittency analysis at FXT $\sqrt{s_{NN}}$ = 3 GeV is ongoing...